Machine Learning-Enabled Joint Antenna Selection and Precoding Design: From Offline Complexity to Online Performance

Thang X. Vu, *Member, IEEE*, Symeon Chatzinotas, *Senior Member, IEEE*, Van-Dinh Nguyen, *Member, IEEE*, Dinh Thai Hoang, *Member, IEEE*, Diep N. Nguyen, *Senior Member, IEEE*, Marco Di Renzo, *Fellow, IEEE*, and Björn Ottersten, *Fellow, IEEE*

***Abstract*— We investigate the performance of multi-user multiple-antenna downlink systems in which a base station (BS) serves multiple users via a shared wireless medium. In order to fully exploit the spatial diversity while minimizing the passive energy consumed by radio frequency (RF) components, the BS is equipped with M RF chains and N antennas, where $M < N$. Upon receiving pilot sequences to obtain the channel state information (CSI), the BS determines the best subset of M antennas for serving the users. We propose a joint antenna selection and precoding design (JASPD) algorithm to maximize the system sum rate subject to a transmit power constraint and quality of service (QoS) requirements. The JASPD algorithm overcomes the non-convexity of the formulated problem via a doubly iterative algorithm, in which an inner loop successively optimizes the precoding vectors, followed by an outer loop that tests all valid antenna subsets. Although approaching (near) global optimality, the JASPD suffers from a combinatorial complexity, which may limit its application in real-time network operations. To overcome this limitation, we propose a learning-based antenna selection and precoding design algorithm (L-ASPA), which employs a deep neural network (DNN) to establish underlaying relations between key system parameters and the selected antennas. The proposed L-ASPD algorithm is robust against the number of users and their locations, the transmit power of the BS, as well as the small-scale channel fading. With a well-trained learning model, it is shown that the L-ASPD algorithm significantly outperforms baseline schemes based on the block diagonalization and a learning-assisted solution for broadcasting systems and achieves a better effective sum rate than that of the JASPA under limited processing time. In addition, we observed that the proposed L-ASPD algorithm can reduce the computation complexity by 95% while retaining more than 95% of the optimal performance.**

***Index Terms*— Multiuser, precoding, antenna selection, machine learning, neural networks, successive convex optimization.**

Manuscript received April 14, 2020; revised August 26, 2020 and December 17, 2020; accepted January 13, 2021. Date of publication January 27, 2021; date of current version June 10, 2021. This work was supported by the European Research Council through the project AGNOSTIC under Grant 742648. This article was presented in part at the 17th International Symposium on Modeling and Optimization in Mobile, Ad Hoc and Wireless Networks (WiOpt 2019). The associate editor coordinating the review of this article and approving it for publication was A. El Gamal. *(Corresponding author: Thang X. Vu.)*

Thang X. Vu, Symeon Chatzinotas, Van-Dinh Nguyen, and Björn Ottersten are with the Interdisciplinary Centre for Security, Reliability and Trust (SnT), University of Luxembourg, 1855 Luxembourg, Luxembourg (e-mail: thang.vu@uni.lu; symeon.chatzinotas@uni.lu; dinh.nguyen@uni.lu; bjorn.ottersten@uni.lu).

Dinh Thai Hoang and Diep N. Nguyen are with the School of Electrical and Data Engineering, University of Technology Sydney, Sydney, NSW 2007, Australia (e-mail: hoang.dinh@uts.edu.au; diep.nguyen@uts.edu.au).

Marco Di Renzo is with Université Paris-Saclay, CNRS, CentraleSupélec, Laboratoire des Signaux et Systémes, 91192 Gif-sur-Yvette, France (e-mail: marco.di-renzo@universite-paris-saclay.fr).

Color versions of one or more figures in this article are available at https://doi.org/10.1109/TWC.2021.3052973.

Digital Object Identifier 10.1109/TWC.2021.3052973

I. Introduction

MULTIPLE-INPUT multiple-output (MIMO) is an enabling technology to deal with the rapidly increasing demand for data-hungry applications in current and future mobile networks. By using a large number of antennas, an MIMO base station is able to send multiple information streams to multiple users simultaneously with negligible inter-user interference. The advantages of MIMO systems, under a proper beamforming design, comprise not only high spectral efficiency but also improved energy efficiency [1]. When the number of antennas in MIMO systems becomes very large, antenna selection (AS) can be employed to improve the performance in terms of both hardware cost and technological aspects [2]. This is due to the fact that the radio frequency (RF) chains are usually much more expensive than antenna elements. More importantly, a proper AS strategy is capable of not only obtaining full spatial diversity but also considerably minimizing the RF chains' energy consumption, hence improving the system energy efficiency [3]. In general, AS is an NP-hard problem whose optimal solution is only guaranteed via exhaustive search, which tries all possible antenna combinations. The high complexity of AS may limit its application in practice, especially in 5G services which usually have stringent latency and real-time decision making requirements [4].

Low-complexity solutions have become necessary to make AS practically feasible, especially for BSs with medium to large numbers of antennas. A block diagonalization-based algorithm is proposed in [5] for multiuser MIMO systems, which selects the best antennas to either minimize the symbol error rate (SER) upper bound or maximize the minimum capacity. This method consecutively eliminates one antenna at a time that imposes the highest energy consumption

in the corresponding orthogonal beamformers. The authors of [6] propose a joint beamforming design and AS algorithm to minimize the multicasting transmit power. By using group sparsity-promoting $l_{1,2}$ norms instead of the l_0 norm, the selected antennas and beamformers can be obtained via an iterative algorithm. The application of $l_{1,2}$ norms is also employed in massive MIMO for minimizing the transmit power [7] and in cell-free MIMO downlink setups for joint access point selection and power allocation [8]. In [9], an AS algorithm based on mirror-prox successive convex approximation (SCA) is proposed for maximizing the minimum rate in multiple-input single-output (MISO) broadcasting systems. A similar SCA-based approach is proposed in [10], [11] for energy efficiency maximization.

Recently, the use of machine learning (ML) in communications systems has attracted much attention [12]–[24]. The main advantage of ML-aided communications lies in the capability of establishing underlying relations between system parameters and the desired objective, hence being able to shift the computation burden in real-time processing to the offline training phase [25], [26]. The authors of [16] propose a beamforming neural network (BNN) for minimizing the transmit power of multiuser MISO systems, which employs convolutional neural networks (CNN) and a supervised-learning method to predict the magnitude and direction of the beamforming vectors. This method is extended in [17], [18] for unsupervised-learning to maximize the system weighted sum-rate. In [19], a deep learning-aided transmission strategy is proposed for single-user MIMO system with limited feed back, which is capable of addressing both pilot-aided training and channel code selection. The authors of [20] develop a deep learning-based beamforming design to maximize the spectral efficiency of a single-user millimeter wave (mmWave) MISO system, which achieves a better spectral efficiency than conventional hybrid beamforming designs. The application of Q-learning is elaborated in [21] to overcome the combinatorial-complexity task of selecting the best channel impulse response in vehicle to infrastructure communications. A similar Q-learning based method is proposed in [23] to solve the joint design of beamforming, power control, and interference coordination of cellular networks. In [22], the authors develop a deep reinforcement learning framework which can autonomously optimize broadcast beams in MIMO broadcast systems based on users' measurements. A common data set for training mmWave MIMO networks is provided in [24] considering various performance metrics.

Towards the learning-aided physical layer design, the application of ML to AS is a promising way to tackle the high complexity of AS [27]–[30]. A joint design for AS and hybrid beamformers for single-user mmWave MIMO is proposed in [27] based on two serial CNNs, in which one CNN is used to predict the selected antennas and another CNN is used to estimate the hybrid beamformers. The authors of [28] propose a multi-class classification approach to tackle the AS problem in single-user MIMO systems based on two classification methods, namely multiclass k-nearest neighbors and support vector machine (SVM). In [29], a neural network-based approach is proposed to reduce the computational complexity of AS for broadcasting. The neural network (NN) is employed to directly predict the selected antennas that maximize the minimum signal to noise ratio among the users. The authors of [30] propose a learning-based transmit antenna selection method to improve the security in the wiretap channel. Therein, two learning-based SVM and naive-Bayes schemes are considered. Although being able to improve the secrecy performance with a reduced feedback overhead, the setup analyzed in [30] is limited to only a single antenna selection.

A. Contributions

In this paper, we investigate the performance of a multiuser MISO downlink system via a joint design of AS and precoding vectors to improve the system sum rate while guaranteeing the users' quality of service (QoS) requirements. Our contributions are as follows:

- First, we develop a joint antenna selection and beamforming design (JASPD) framework to maximize the *effective* system sum rate, which accounts for the time overhead spent on both channel estimation and computational processing, subject to users' QoS requirements and a limited transmit power budget. The proposed JASPD works in an iterative manner, which first optimizes the beamforming vectors for a given antenna subset, and then selects the best antenna subset.
- Second, to tackle the non-convexity in optimizing the beamforming vectors of JASPD, we propose two iterative optimization algorithms based on semidefinite relaxation (SDR) and SCA methods. The convergence of the proposed iterative algorithms to at least a local optimum is theoretically guaranteed.
- Third, we propose a learning-based antenna selection and precoding design (L-ASPD) algorithm to overcome the high computational complexity of AS, which employs a deep neural network (DNN) to capture and reveal the relationship between the system parameters and the selected antennas via an offline training process. More importantly, our leaning model is robust against the channel fading and the number of users and their locations. Compared to existing works, which either study single-user MIMO systems [27], [28], a single beamformer for broadcasting [29] or a single antenna selection [30], we consider a more general multi-user system.
- Finally, extensive simulation results show that, under the same limited processing time, the proposed L-ASPD algorithm outperforms the JASPD algorithm and significantly outperforms existing AS schemes based on model-based [5] and ML-aided [29] designs. We observed that the L-ASPD algorithm can achieve more than 95% of the optimal sum rate while reducing more than 95% the computational time.

The rest of the paper is organized as follows. Section II presents the system model and key parameters. Section III develops two iterative optimization algorithms used in the JASPD. Section IV introduces a ML-aided joint design to accelerate real-time processing. Section V demonstrates the

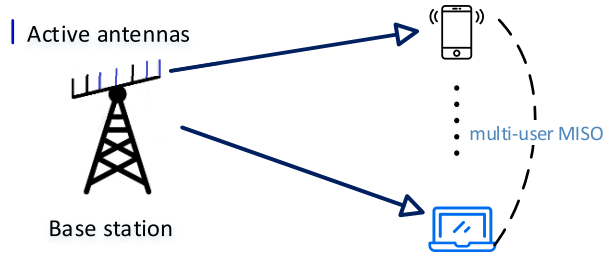

Fig. 1. Diagram of multiuser MISO system. A subset of antennas is selected for data transmission.

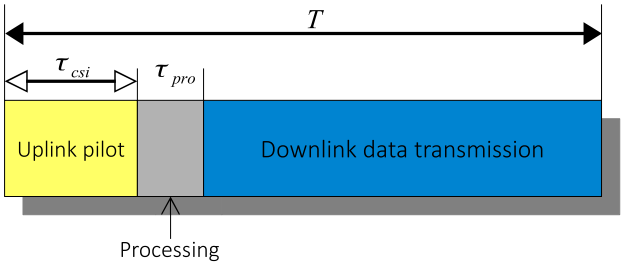

Fig. 2. Block diagram of one transmission block.

effectiveness of the proposed algorithms via numerical results. Finally, Section IV concludes the paper.

Notations: The superscript $(.)^T$, $(.)^H$ and $\mathrm{Tr}(.)$ stand for the transpose, Hermitian transpose, and trace operation, respectively. $\binom{n}{k}$ represents the binomial coefficients. $|.|$ and $\|.\|$ denote the cardinality and the l_2-norm of a set, respectively.

II. System Model

We consider a multiuser MISO downlink system operated in time division duplex (TDD) mode, in which a multi-antenna base station (BS) servers K single-antenna users in the same frequency resource,[1] as depicted in Fig. 1. The BS is equipped with M RF chains and N antennas, where $N > M \geq K$. The motivation of having more antennas than the number of RF chains is that the BS can i) fully exploit spatial diversity gains and ii) minimize the static energy consumed by hardware components [3], e.g., RF chains and amplifiers. The system operates in a quasi-static block fading channel in which the channel gains are constant within on block and independently change from one block to another. Before sending data to the users, the BS needs to acquire the channel state information (CSI) via pilot-aided channel estimation[2] in order to perform reprocessing, e.g., beamforming and power allocation.

Fig. 2 illustrates the three phases in one transmission block. Let T and τ_{csi} denote the block duration and channel estimation time, both expressed in terms of channel use (c.u.), respectively. The block duration is determined by the system coherence time. Assuming mutually orthogonal pilot sequences across the users, the channel estimation time is $\tau_{csi} = K(\lfloor N/M \rfloor + 1)$ c.u., where $\lfloor x \rfloor$ denotes the largest integer not exceeding x. Unlike most of previous works that ignore the processing time, we consider the general case in which the processing time takes place in τ_{pro} (c.u.). In practice, the value of τ_{pro} largely depends on the beamforming techniques and the hardware capability.

Let $\boldsymbol{h}_k \in \mathbb{C}^{1\times N}$ denote the channel vector from the BS's antennas to user k, including the pathloss. We assume that full CSI is available at the BS. Because there are only $M < N$ RF chains, the BS has to determine an optimal subset of M antennas for sending data to the users. Let $\mathcal{A} = \{a_1, a_2, \ldots, a_M\}, a_m \in [N] \triangleq \{1, 2, \ldots, N\}$, be a subset of M antennas (out of N), and let $\boldsymbol{\mathcal{A}}$ be the collection of all possible antenna subsets. By definition, we have $|\mathcal{A}| = M$ and $|\boldsymbol{\mathcal{A}}| = \binom{N}{M}$.

Denote by $\boldsymbol{h}_{k,\mathcal{A}} \in \mathbb{C}^{1\times M}$ the channel vector from active antennas in a subset $\mathcal{A}$ to user k, i.e., $\boldsymbol{h}_{k,\mathcal{A}} = [h_k[a_1], h_k[a_2], \ldots, h_k[a_M]]$, where $a_m \in \mathcal{A}$ and $h_k[n]$ is the n-th element of $\boldsymbol{h}_k$. Before serving the users, the BS first precodes the data to suppress inter-user interference. Let $\boldsymbol{w}_{k,\mathcal{A}} \in \mathbb{C}^{M\times 1}$ be the precoding vector for user k corresponding to the selected antenna subset $\mathcal{A}$. The received signal at user k is

$$y_{k,\mathcal{A}} = \boldsymbol{h}_{k,\mathcal{A}}\boldsymbol{w}_{k,\mathcal{A}}x_k + \sum\nolimits_{i\neq k}\boldsymbol{h}_{k,\mathcal{A}}\boldsymbol{w}_{i,\mathcal{A}}x_i + n_k, \quad (1)$$

where n_k is the Gaussian noise with zero mean and variance σ^2. The first term in (1) is the desired signal, and the second term is the inter-user interference.

By considering interference as noise, the *effective achievable rate* of user k is

$$R_k(\mathcal{A}) = B\left(1 - \frac{\tau_{csi} + \tau_{pro}}{T}\right) \times \log_2\left(1 + \frac{|\boldsymbol{h}_{k,\mathcal{A}}\boldsymbol{w}_{k,\mathcal{A}}|^2}{\sum_{i\neq k}|\boldsymbol{h}_{k,\mathcal{A}}\boldsymbol{w}_{i,\mathcal{A}}|^2 + \sigma^2}\right), \quad \forall k, \quad (2)$$

where B is the shared channel bandwidth and $1 - \frac{\tau_{csi}+\tau_{pro}}{T}$ accounts for the actual time for data transmission. The total transmit power[3] is $\sum_{k=1}^{K}\|\boldsymbol{w}_{k,\mathcal{A}}\|^2$.

Remark 1: It is observed from (2) that the effective data rate is determined not only by the precoding vectors $\boldsymbol{w}_{k,\mathcal{A}}$ but also by the channel estimation and processing times. In particular, spending more time on either channel estimation or processing will degrade the effective transmission rate.

III. Optimal Antenna Selection and Precoding Design

In this section, we develop a joint antenna selection and precoding design to maximize the system sum rate while satisfying the minimum QoS requirements and limited power budget. The joint optimization problem can be formulated

[1]In practice the whole bandwidth is divided into multiple sub-frequency bands. The proposed scheme is directly applied to each band.

[2]The system is assumed to operate above certain SNR levels in which the CSI can be accurately estimated.

[3]The energy consumed by hardware components is excluded since it is constant and does not affect the precoding design.

as follows:

$$\text{P0}: \quad \underset{\mathcal{A}\in\boldsymbol{\mathcal{A}},\{\boldsymbol{w}_{k,\mathcal{A}}\}}{\texttt{maximize}} \ \sum\nolimits_{k=1}^{K} R_k(\mathcal{A}) \quad (3)$$
$$\texttt{s.t.} \ \ R_k(\mathcal{A}) \geq \eta_k, \quad \forall k,$$
$$\sum\nolimits_{k=1}^{K} \|\boldsymbol{w}_{k,\mathcal{A}}\|^2 \leq P_{tot},$$

where $R_k(\mathcal{A})$ is given in (2), P_{tot} is the total transmit power budget at the BS, and η_k is the QoS requirement for user k. In problem (3), the first constraint is to satisfy the minimum user QoS requirement and the second constraint states that the total transmit power can not exceed the power budget. We note that the problem formulation in (3) can be directly extended to the weighted sum rate metric with the weights that are used as part of the training input.

In general, problem (3) is a mixed binary non-linear problem where the binary variables of the activated antennas are strongly coupled with the continuous variables of the precoding vectors. Because the precoding vectors are designed for a given selected antenna subset, problem P0 can be reformulated in an iterative form as follows:

$$\underset{\mathcal{A}\in\boldsymbol{\mathcal{A}}}{\texttt{maximize}} \ \ \text{P1}(\mathcal{A}), \quad (4)$$

where $\text{P1}(\mathcal{A})$ is the precoding design problem for the candidate antenna subset $\mathcal{A}$, which is defined as follows

$$\text{P1}(\mathcal{A}): \ \underset{\{\boldsymbol{w}_{k,\mathcal{A}}\}}{\texttt{Max}} \ \ \bar{B}\sum_{k=1}^{K}\log_2\Big(1+\frac{|\boldsymbol{h}_{k,\mathcal{A}}\boldsymbol{w}_{k,\mathcal{A}}|^2}{\sum_{i\neq k}|\boldsymbol{h}_{k,\mathcal{A}}\boldsymbol{w}_{i,\mathcal{A}}|^2+\sigma^2}\Big) \quad (5)$$

$$\texttt{s.t.} \ \ \bar{B}\log_2\Big(1+\frac{|\boldsymbol{h}_{k,\mathcal{A}}\boldsymbol{w}_{k,\mathcal{A}}|^2}{\sum_{i\neq k}|\boldsymbol{h}_{k,\mathcal{A}}\boldsymbol{w}_{i,\mathcal{A}}|^2+\sigma^2}\Big)\geq\eta_k, \quad \forall k, \quad (5a)$$

$$\sum\nolimits_{k=1}^{K}\|\boldsymbol{w}_{k,\mathcal{A}}\|^2 \leq P_{tot}, \quad (5b)$$

where $\bar{B}\triangleq B(1-\frac{\tau_{csi}+\tau_{pro}}{T})$ and we have used (2) for $R_k(\mathcal{A})$.

If problem $\text{P1}(\mathcal{A})$ can be solved optimally, then the optimal solution of P0 can be obtained via an exhaustive search in (4), which test all possible antenna subsets. Unfortunately, solving problem $\text{P1}(\mathcal{A})$ is challenging due to the non-concavity of the objective function and the non-convexity of the first constraint.

In the following, we propose two solutions based on SDR and SCA methods to tackle the non-convexity of the beamforming vectors design in Section III-A. We then describe the proposed JASPD algorithm and analyze its complexity in Section III-B.

A. Near Optimal Beamforming Design for Selected Antennas

In this subsection, we design the beamforming vectors to maximize the system sum rate for a selected antenna subset. In the following, we propose two methods to solve (5).

1) Semidefinite Relaxation-Based Solution: Semidefinite-based formulation is an efficient method to design the beamforming vectors of wireless systems, which converts quadratic terms into linear ones by lifting the original variable domain into a higher-dimensional space. We adopt the semidefinite method to deal with the signal-to-noise-plus-interference-ratio (SINR) term in both the objective function and the first constraint. Define a new set of variables $\boldsymbol{W}_k=\boldsymbol{w}_{k,\mathcal{A}}\boldsymbol{w}_{k,\mathcal{A}}^H\in\mathbb{C}^{M\times M}$, and denote $\boldsymbol{H}_k\triangleq\boldsymbol{h}_{k,\mathcal{A}}^H\boldsymbol{h}_{k,\mathcal{A}}$. It is straightforward to verify that $|\boldsymbol{h}_{k,\mathcal{A}}\boldsymbol{w}_{l,\mathcal{A}}|^2=\boldsymbol{h}_{k,\mathcal{A}}\boldsymbol{w}_{l,\mathcal{A}}\boldsymbol{w}_{l,\mathcal{A}}^H\boldsymbol{h}_{k,\mathcal{A}}^H=\text{Tr}(\boldsymbol{H}_k\boldsymbol{W}_l)$ and $\|\boldsymbol{w}_{k,\mathcal{A}}\|^2=\text{Tr}(\boldsymbol{W}_k)$.

By introducing arbitrary positive variables $\{x_k\}_{k=1}^K$, we can reformulate problem (5) as follows:

$$\underset{\boldsymbol{W},\boldsymbol{x}}{\texttt{maximize}} \ \ \frac{\bar{B}}{\log(2)}\sum\nolimits_{k=1}^{K}x_k \quad (6)$$

$$\texttt{s.t.} \ \ \log\Big(1+\frac{\text{Tr}(\boldsymbol{H}_k\boldsymbol{W}_k)}{\sum_{i\neq k}\text{Tr}(\boldsymbol{H}_k\boldsymbol{W}_i)+\sigma^2}\Big)\geq x_k, \quad \forall k, \quad (6a)$$

$$x_k\geq\frac{\eta_k\log(2)}{\bar{B}}, \quad \forall k, \quad (6b)$$

$$\sum\nolimits_{k=1}^{K}\text{Tr}(\boldsymbol{W}_k)\leq P_{tot}, \quad (6c)$$
$$\text{rank}(\boldsymbol{W}_k)=1, \quad \forall k,$$

where we use short-hand the notation $\boldsymbol{W}$ and $\boldsymbol{x}$ for $(\boldsymbol{W}_1,\ldots,\boldsymbol{W}_K)$ and $(x_1,\ldots,x_K)$, respectively.

The equivalence between (6) and (5) can be verified as the equality holds in (6a) at the optimum. It is observed that the objective is a linear function and constraints (6b) and (6c) are convex. Thus, the challenge in solving problem (6) lies in (6a) and the rank-one constraint. While the latter constraint can be efficiently coped with by using the relaxation method followed by randomization if needed [32], dealing with the former constraint is more difficult.

In the next step, we introduce the slack variables $\{y_k\}_{k=1}^K$ and reformulate constraint (6a) as

$$\log\Big(\sigma^2+\sum\nolimits_{i=1}^{K}\text{Tr}(\boldsymbol{H}_k\boldsymbol{W}_i)\Big)\geq x_k+y_k, \quad (7)$$
$$\sigma^2+\sum\nolimits_{i\neq k}\text{Tr}(\boldsymbol{H}_k\boldsymbol{W}_i)\leq e^{y_k}. \quad (8)$$

Because the function $\log()$ is concave, constraint (7) is convex. However, since the function $\exp(.)$ is convex, constraint (8) is unbounded. To overcome this difficulty, we employ the inner approximation method, which uses the first-order approximation of e^{y_k} at the right hand side of (8). As a result, the approximated problem of (6) can be formulated as follows:

$$\text{P2}(\boldsymbol{y}_0): \ \underset{\boldsymbol{W},\boldsymbol{x},\boldsymbol{y}}{\texttt{maximize}} \ \ \frac{\bar{B}}{\log(2)}\sum\nolimits_{k=1}^{K}x_k \quad (9)$$
$$\texttt{s.t.} \ \ (6\text{b});(6\text{c});(7); \ \text{rank}(\boldsymbol{W}_k)=1, \quad \forall k,$$
$$\sigma^2+\sum\nolimits_{i\neq k}\text{Tr}(\boldsymbol{H}_k\boldsymbol{W}_i)\leq e^{y_{0k}}(y_k-y_{0k}+1), \quad \forall k, \quad (9a)$$

where $\boldsymbol{y}\triangleq\{y_k\}_{k=1}^K$ and $\boldsymbol{y}_0$ is any feasible value of $\boldsymbol{y}$ that satisfies constraint (8).

It is evident that, for a given $\boldsymbol{y}_0$, the objective and constraints of problem (9) are convex except for the rank one constraint. This suggests to solve (9) by the semi-definite relaxation (SDR) method [32] which ignores the rank one constraint and can be solved in an efficient manner by standard solvers, e.g., CVX. Because $e^{y_0}(y-y_0+1)\leq e^y, \forall y_0$, the approximated problem (9) always gives a suboptimal solution of the original problem (6).

Algorithm 1 Iterative Algorithm to Solve (6)

1: Initialize $\boldsymbol{y}_0$, ϵ, $X_{\rm old}$ and `error`.
2: **while** `error` $> \epsilon$ **do**
3: Solve the SDR of (9) by dropping the rank-one constraint to obtain $\{\boldsymbol{W}_{\star k}, x_{\star k}, y_{\star k}\}_{k=1}^K$
4: Compute `error` $= \frac{\bar{B}}{\log(2)}|\sum_{k=1}^K x_{\star k} - X_{\rm old}|$
5: Update $X_{\rm old} \leftarrow \frac{\bar{B}}{\log(2)}\sum_{k=1}^K x_{\star k}$; $y_{0k} \leftarrow y_{\star k}, \forall k$

It is worth noting that the optimal solution of problem (9) is largely determined by the parameters $\boldsymbol{y}_0$. Thus, it is crucial to select appropriate values $\boldsymbol{y}_0$ such that the solution of (9) is close to the optimal solution of (6). As such, we propose an iterative optimization algorithm to improve the performance of problem (9), shown in Algorithm 1. The premise behind the proposed algorithm is to better estimate $\boldsymbol{y}_0$ through iterations.

Proposition 1 (Convergence of Algorithm 1): The sequence of the objective values generated by Algorithm 1 in solving the SDR of problem P2($\boldsymbol{y}_0$) is non-decreasing.

The proof of Proposition 1 is shown in Appendix A. Although not guaranteeing the global optimum of problem (6), Proposition 1 justifies the convergence to at least a local optimum of the proposed iterative algorithm.[4]

Remark 2 (Initialization of Algorithm 1): The execution of Algorithm 1 requires the initial values $y_{0k}, \forall k$. Therefore, it requires an efficient way to find these initial values before tackling problem (9). To this end, we start by solving the feasibility problem below:

$$\begin{aligned} &\texttt{Find} \quad \boldsymbol{W} \\ &\texttt{s.t.} \quad \frac{\mathrm{Tr}(\boldsymbol{H}_k\boldsymbol{W}_k)}{2^{\eta_k/\bar{B}}-1} \geq \sum\nolimits_{i\neq k}\mathrm{Tr}(\boldsymbol{H}_k\boldsymbol{W}_i) + \sigma^2, \quad \forall k, \\ &\qquad \sum\nolimits_{k=1}^K \mathrm{Tr}(\boldsymbol{W}_k) \leq P_{tot}, \end{aligned} \tag{10}$$

which is convex. Then the initial values are computed as $y_{0k} = \log(\sum_{i\neq k}\mathrm{Tr}(\boldsymbol{H}_k\boldsymbol{W}_i^*) + \sigma^2), \forall k$, where $\boldsymbol{W}_k^*$ is the solution of (10).

Remark 3 (Randomization): The solution in (9) is based on the SDR which sometimes violates the rank-one constraint. In such cases, Gaussian randomization can be adopted. Details on Gaussian randomization are available in [32]. Our simulation results show that more than 99% of the times Algorithm 1 can output rank-one solutions.

2) Reformulation Based on Difference of Convex: The SDR-based reformulation in the previous subsection leverages the non-convexity of the original problem by working in a higher dimensional domain, which requires more memory. In this subsection, we solve (5) based on a difference-of-convex (DC) reformulation directly on the original variable domain.

By introducing arbitrary positive variables $\boldsymbol{u} \triangleq \{u_k\}_{k=1}^K$, we can reformulate problem (5) as follows:

$$\underset{\boldsymbol{w},\boldsymbol{u}}{\texttt{Maximize}} \quad \bar{B}\sum\nolimits_{k=1}^K \log_2(1+u_k) \tag{11}$$

$$\begin{aligned} \texttt{s.t.} \quad & \frac{|\boldsymbol{h}_{k,\mathcal{A}}\boldsymbol{w}_{k,\mathcal{A}}|^2}{\sum_{i\neq k}|\boldsymbol{h}_{k,\mathcal{A}}\boldsymbol{w}_{i,\mathcal{A}}|^2+\sigma^2} \geq u_k, \quad \forall k, && \text{(11a)} \\ & u_k \geq \bar{\eta}_k, \quad \forall k, && \text{(11b)} \\ & \sum\nolimits_{k=1}^K \|\boldsymbol{w}_{k,\mathcal{A}}\|^2 \leq P_{tot}, && \text{(11c)} \end{aligned}$$

where $\bar{\eta}_k \triangleq 2^{\eta_k/\bar{B}} - 1$ and $\boldsymbol{w}$ is a short-hand notation for $(\boldsymbol{w}_{1,\mathcal{A}}, \ldots, \boldsymbol{w}_{K,\mathcal{A}})$. The equivalence between (11) and (5) can be verified since constraint (11a) holds with equality at the optimum.

As the denominator of the left-hand-side of (11a) is positive, it can be rewritten as

$$\frac{|\boldsymbol{h}_{k,\mathcal{A}}\boldsymbol{w}_{k,\mathcal{A}}|^2}{u_k} \geq \sum\nolimits_{i\neq k}|\boldsymbol{h}_{k,\mathcal{A}}\boldsymbol{w}_{i,\mathcal{A}}|^2 + \sigma^2. \tag{12}$$

An important observation from (12) is that $\frac{|\boldsymbol{h}_{k,\mathcal{A}}\boldsymbol{w}_{k,\mathcal{A}}|^2}{u_k}$ is a convex function of $\boldsymbol{w}_{k,\mathcal{A}}$ and u_k (see Appendix B). Therefore, (12) has the form of a DC representation, which suggests an efficient way to solve (11a). In particular, let $\hat{\boldsymbol{w}}_{k,\mathcal{A}}, \hat{u}_k$ be any feasible solution of (11), we can approximate (12) by using the first order approximation of the left-hand-side of (12), stated as

$$\begin{aligned} \sum_{i\neq k}\boldsymbol{w}_{k,\mathcal{A}}^H\boldsymbol{H}_k\boldsymbol{w}_{i,\mathcal{A}} + \sigma^2 \leq{}& \frac{\boldsymbol{w}_{k,\mathcal{A}}^H\left(\boldsymbol{H}_k+\boldsymbol{H}_k^T\right)\hat{\boldsymbol{w}}_{k,\mathcal{A}}}{\hat{u}_k} \\ & -u_k\frac{\hat{\boldsymbol{w}}_{k,\mathcal{A}}^H\boldsymbol{H}_k\hat{\boldsymbol{w}}_{k,\mathcal{A}}}{\hat{u}_k^2} + \frac{\hat{\boldsymbol{w}}_{k,\mathcal{A}}^H\left(\boldsymbol{H}_k-\boldsymbol{H}_k^T\right)\hat{\boldsymbol{w}}_{k,\mathcal{A}}}{\hat{u}_k}, \end{aligned} \tag{13}$$

which is convex in $\boldsymbol{w}_{k,\mathcal{A}}$ and u_k, where $\boldsymbol{H}_k = \boldsymbol{h}_{k,\mathcal{A}}^H\boldsymbol{h}_{k,\mathcal{A}}$.

By using (13) as an approximation of (11a), problem (11) can be approximated as

$$\begin{aligned} \mathrm{P3}(\hat{\boldsymbol{w}},\hat{\boldsymbol{u}}): \ & \underset{\boldsymbol{w},\boldsymbol{u}}{\texttt{Maximize}} \quad \bar{B}\sum\nolimits_{k=1}^K \log_2(1+u_k) \\ & \texttt{s.t.} \quad \text{(11b)}; \ \text{(11c)}; \ \text{(13)}. \end{aligned} \tag{14}$$

For given $\hat{\boldsymbol{w}}_{k,\mathcal{A}}, \hat{x}_k$, the objective function in (14) is concave and the constraints are convex, hence it can be solved in an efficient manner by standard solvers, e.g., CVX. Because the right-hand-side of (13) is always less than or equal to $\frac{\boldsymbol{w}_{k,\mathcal{A}}^H\boldsymbol{H}_k\boldsymbol{w}_{k,\mathcal{A}}}{u_k}$, the approximated problem (14) always gives a suboptimal solution of the original problem (11).

In order to reduce the performance gap between the approximated problem (14) and the original problem (11), we propose Algorithm 2 which consists of solving a sequence of SCA problems. The premise behind the proposed algorithm is to better select the parameters $\hat{\boldsymbol{w}}_{k,\mathcal{A}}, \hat{u}_k$ through iterations.

Algorithm 2 Iterative Algorithm to Solve (11)

1: Initialize $\hat{\boldsymbol{w}}_{k,\mathcal{A}}, \hat{u}_k$, ϵ, $X_{\rm old}$ and `error`.
2: **while** `error` $> \epsilon$ **do**
3: Solve problem P3($\hat{\boldsymbol{w}}_{k,\mathcal{A}}, \hat{u}_k$) in (14) to obtain $\boldsymbol{w}_k^\star, u_k^\star, \forall k$
4: Compute `error` $= |\bar{B}\sum_{k=1}^K \log_2(1+u_k^\star) - X_{\rm old}|$
5: Update $X_{\rm old} \leftarrow \bar{B}\sum_{k=1}^K \log_2(1+u_k^\star)$; $\hat{\boldsymbol{w}}_{k,\mathcal{A}} \leftarrow \boldsymbol{w}_k^\star$; $\hat{u}_k \leftarrow u_k^\star, \forall k$

[4]The study of the performance gap to the global optimum is postponed to a future work.

Algorithm 3 Exhaustive Search Based Joint Antenna Selection and Precoding Design

Inputs: $\boldsymbol{H}, P_{tot}, \{\eta_k\}_{k=1}^K$. **Outputs**: $C_{opt}, \mathcal{A}_{opt}, \boldsymbol{W}_{opt}$

Construct the super group $\boldsymbol{\mathcal{A}} = \{\mathcal{A} \mid \mathcal{A} \subset [N], |\mathcal{A}| = M\}$
Initialize $C_{opt} = 0$
for $i = 1 : |\boldsymbol{\mathcal{A}}|$ **do**
    $\mathcal{A} = \boldsymbol{\mathcal{A}}[i]$
    Apply Algorithm 1 or Algorithm 2 on the current antenna subset $\mathcal{A}$ to obtain the optimal $X_{old}(\mathcal{A})$ and $\boldsymbol{W}_\star(\mathcal{A})$
If $C_{opt} < X_{old}(\mathcal{A})$
    $C_{opt} \leftarrow X_{old}(\mathcal{A})$; $\mathcal{A}_{opt} \leftarrow \mathcal{A}$; $\boldsymbol{W}_{opt} = \boldsymbol{W}_\star(\mathcal{A})$.

Remark 4 (Initialization of Algorithm 2): Finding a feasible point is always essential in the SCA. Intuitively, one can think about the feasibility problem of (5), which is stated as

$$\underset{\{\boldsymbol{w}_{k,\mathcal{A}}\}}{\texttt{Maximize}} \ 1 \tag{15}$$

$$\texttt{s.t.} \ \ \frac{1}{\bar{\eta}_k}|\boldsymbol{h}_{k,\mathcal{A}}\boldsymbol{w}_{k,\mathcal{A}}|^2 \geq \sum_{i\neq k}|\boldsymbol{h}_{k,\mathcal{A}}\boldsymbol{w}_{i,\mathcal{A}}|^2 + \sigma^2, \quad \forall k, \tag{15a}$$

$$\sum\nolimits_{k=1}^K \|\boldsymbol{w}_{k,\mathcal{A}}\|^2 \leq P_{tot}. \tag{15b}$$

However, since both sides of (15a) are convex, this constraint is unbounded. Therefore, finding a feasible point by solving (15) is not efficient. Instead, we adopt (10) as the means to find initial values $\hat{\boldsymbol{w}}, \hat{\boldsymbol{u}}$. In particular, from the optimal outputs of Algorithm 3 $\boldsymbol{W}_{\star k}, \forall k$, the solution of the convex problem (10), we obtain the corresponding feasible precoding vectors $\boldsymbol{w}_{\star k}$. Then, we assign $\hat{\boldsymbol{w}}_k = \boldsymbol{w}_{\star k}$ and $\hat{u}_k = \frac{|\boldsymbol{h}_{k,\mathcal{A}}\boldsymbol{w}_{\star k}|^2}{\sum_{i\neq k}|\boldsymbol{h}_{k,\mathcal{A}}\boldsymbol{w}_{\star i}|^2+\sigma^2}$.

B. JASPD Algorithm and Complexity Analysis

Once the precoding vectors have been optimized for each antenna subset, i.e., problem (5) is solved, we can tackle the original optimization problem (3) via Algorithm 3.

The proposed JASPD algorithm consists of two loops: the outer loop tries all valid antenna subsets, and the inner loop optimizes the precoding vectors iteratively. While the complexity of the inner loop is relatively reasonable since (the SDR of) problem (9) (or problem (14)) is convex [36], the complexity of the outer iteration increases combinatorially with the number of antennas. In fact, the JASPD has to examine all $\binom{N}{M}$ candidates for the selected antennas. As an example, for $N = 20, M = 8$, there are 125970 possible antenna subsets to be tested, each of which imposes an inner loop in Algorithm 1 or Algorithm 2. Although guaranteeing the maximal achievable rate, the proposed JASPD algorithm suffers an exponential complexity due to the selection process. Its high computation time may limit its applicability in practice and may degrade the effective rate (see (2)). In the next section, we propose a low-complexity joint design to overcome the computation burden of the antenna selection process.

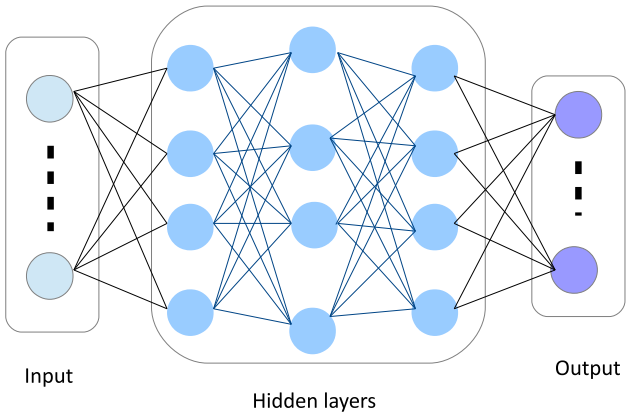

Fig. 3. Illustration of a DNN with three hidden layers.

IV. Accelerating the Optimization: A Deep Learning-Based Approach

In this section, we exploit recent advances in machine learning to overcome the major high-complexity limitation of the selection process by proposing a learning-based antenna selection and precoding design (L-ASPD) algorithm. The premise behind the proposed L-ASPD algorithm is to exploit machine-learning based predictions to help the optimal algorithm to tackle the most difficult and time-consuming part in the optimization. In particular, the L-ASPD algorithm first predicts potential subsets of antennas, which are much smaller than $\binom{N}{M}$.

We deploy DNN as the learning model to establish underlaying relations between the system parameters (inputs) and the selected antenna subset. The DNN consists of three main parts: one input layer, one output layer and hidden layers, as depicted in Fig. 3. Based on the labeled data, the DNN optimizes the learning parameters in order to minimize the prediction error, e.g., cost function. The L-ASPD algorithm is implemented via 3 steps: i) offline training data generation, ii) building the learning model, and iii) real-time prediction.

A. Training Data Generation

Since the communication between the BS and the users is specified by the channel gains, the transmit power budget and noise power, they are essential for the learning model. Let $\boldsymbol{H} = [\boldsymbol{h}_1^H, \ldots, \boldsymbol{h}_K^H]^H \in \mathbb{C}^{K\times N}$ denote the channel coefficients from the BS's antennas to all users. Since the number of users can be arbitrary between 1 and M (the number of RF chains), the channel matrix $\boldsymbol{H}$ is first zero-padded to obtain the standard size $\bar{\mathbf{H}} = [\boldsymbol{H}^H, \mathbf{0}_{N\times(M-K)}]^H \in \mathbb{C}^{M\times N}$. Because the DNN accepts only real-value inputs, the original complex representation of the channel matrix is invalid. One can stack the real and imaginary parts of $\bar{\mathbf{H}}$ and use them as the training input to the DNN [29]. However, we observe that such method is not efficient to our problem because it does not directly capture inter-user interference - the major limiting factor in multiuser systems. As the inter-user interference is determined by the cross-product of the channel vectors of two users, we choose $\boldsymbol{x} = \frac{P_{tot}}{\sigma^2}\text{abs}(\text{vec}(\bar{\mathbf{H}}\bar{\mathbf{H}}^H)) \in \mathbb{R}^{M^2\times 1}$ as the

TABLE I
STEPS TO GENERATE TRAINING SAMPLES FOR L-ASPD

1.	**For** $t = 1 : N_S$
2.	Generate a random number of users K between $[1, M]$.
3.	Generate random locations of these K users between 50 and 300m from the BS. Calculate the pathloss.
4.	Generate a channel matrix $\boldsymbol{H} \in \mathbb{C}^{K\times N}$, including the pathloss.
	Output sample generation
5.	Run JASPD algorithm to find the best antenna subset.
6.	Compute the binary output vector $\boldsymbol{b}_t$ with only a single non-zero element corresponding to the selected subset.
	Input sample generation
5.	Zero-padding: $\bar{\mathbf{H}} = [\boldsymbol{H}^H, \mathbf{0}_{N\times(M-K)}]^H$.
6.	Calculate $\boldsymbol{x}_t = \frac{P_{tot}}{\sigma^2}\text{abs}(\text{vec}(\bar{\mathbf{H}}^H\bar{\mathbf{H}}))$; $\boldsymbol{x}_t = \frac{\boldsymbol{x}_t}{\max(\boldsymbol{x}_t)}$.
7.	**Endfor**

training input. It is worth noting that the training input $\boldsymbol{x}$ is robust against the number of users and pathloss, as well as the BS's transmit power. Last but not least, $\boldsymbol{x}$ needs to be normalized before being fed to the DNN, i.e., $\boldsymbol{x} = \frac{\boldsymbol{x}}{\max(\boldsymbol{x})}$.

Once the input sample is given, we need to define the output, which is the selected antenna combination that provides the maximum objective function in (3). For each training input $\boldsymbol{x}$, we define an output vector $\boldsymbol{b} \in \{0,1\}^{\binom{N}{M}\times 1}$ that consists of all possible antenna subsets. $b[n] = 1$ if the n-th subset is selected, otherwise $b[n] = 0$. Because we are interested in selecting only one subset, we have $\|\boldsymbol{b}\|_0 = 1$. In order to compute $\boldsymbol{b}$, for each channel realization $\boldsymbol{H}$ (corresponding to $\boldsymbol{x}$), we run the proposed JASPD algorithm to find the best antenna subset $\mathcal{A}^\star$ and then assign the output element $b[n^\star] = 1$ corresponding to $\mathcal{A}^\star$. Denote by N_S the number of samples used to train the learning model. The total training input is aggregated in the input matrix $\boldsymbol{X} = [\boldsymbol{x}_1, \boldsymbol{x}_2, \ldots, \boldsymbol{x}_{N_S}]$, where $\boldsymbol{x}_t$ is the t-th input sample. Similarly, the training output matrix is $\boldsymbol{B} = [\boldsymbol{b}_1, \ldots, \boldsymbol{b}_{N_S}]$, where $\boldsymbol{b}_t$ is the t-th output sample corresponding to the input sample $\boldsymbol{x}_t$. The steps for generating the training samples are listed in Table I. We note that the JASPD algorithm considered in Table I is used for generating training samples and is executed off-line. Once the DNN is well-trained, it is used only for the selected antenna subsets in the real-time prediction phase.

B. Building the Learning Model

When the training data is available, it is used to train the DNN with the learning parameter $\boldsymbol{\Theta}$. For an L-layer DNN, we have $\boldsymbol{\Theta} = [\boldsymbol{\theta}_1, \ldots, \boldsymbol{\theta}_L]$, where $\boldsymbol{\theta}_l \in \mathbb{R}^{N_l\times 1}, 1 \le l \le L$, is the learning parameters in the l-th layer, and N_l is the number of nodes in the l-th layer. As the most popular and efficient candidate for classification problems, we employ a sigmoid-family $\texttt{tansig}(z) = 2(1 + e^{-2z})^{-1} - 1$ as the activation function for the hidden layers and the soft-max as the activation function for the output layer. The learning phase can be done via the minimization of the prediction error

$$\begin{aligned}&\Delta(\boldsymbol{\Theta})\\ &= \frac{1}{N_S}\| - \text{Tr}(\boldsymbol{B}^T\log(f_{\boldsymbol{\Theta}}(\boldsymbol{X})))\\ &\quad -\text{Tr}(\bar{\boldsymbol{B}}^T\log(1-f_{\boldsymbol{\Theta}}(\boldsymbol{X})))\ \|^2 + \frac{\lambda}{2N_S}\sum\nolimits_{l=1}^{L}\ \|\ \boldsymbol{\theta}_l\ \|^2, \quad (16)\end{aligned}$$

where λ is the regulation parameter, $\bar{\boldsymbol{B}} = \mathbf{1} - \boldsymbol{B}$, and $f_{\boldsymbol{\Theta}}(\boldsymbol{X})$ is the prediction of the output layer.

Algorithm 4 Proposed L-ASPD Algorithm

Inputs: $\boldsymbol{\Theta}$, $\boldsymbol{H}, P_{tot}, \{\eta_k\}_{k=1}^K$. **Outputs**: $C_{opt}, \mathcal{A}_{opt}, \boldsymbol{w}_{opt}$
1: Construct $\boldsymbol{x} = \frac{P_{tot}}{\sigma^2}\text{abs}(\text{vec}(\boldsymbol{H}^H\boldsymbol{H}))^2$; $\boldsymbol{x}_{\text{norm}} = \frac{\boldsymbol{x}}{\max(\boldsymbol{x})}$
2: Apply $\boldsymbol{x}_{\text{norm}}$ to the learned model $\boldsymbol{\Theta}$ to predict $\boldsymbol{\mathcal{K}}_S$
3: Initialize $C_{opt} = 0$
4: **for** $\mathcal{A} \in \boldsymbol{\mathcal{K}}_S$
5: Apply Algorithm 1 or 2 on the current subset $\mathcal{A}$ to
6: obtain the optimal $X_{old}(\mathcal{A})$ and $\boldsymbol{w}_{\star,\mathcal{A}}$
7: **if** $C_{opt} < X_{old}(\mathcal{A})$
8: $C_{opt} = X_{old}(\mathcal{A})$; $\mathcal{A}_{opt} \leftarrow \mathcal{A}$; $\boldsymbol{w}_{opt} \leftarrow \boldsymbol{w}_{\star,\mathcal{A}}$.

C. Real-Time Prediction

When the DNN has been well trained, it is ready to provide real-time and highly accurate predictions. From the current channel coefficient matrix $\boldsymbol{H}$, we construct $\boldsymbol{x} = \frac{P_{tot}}{\sigma^2}\text{abs}(\text{vec}(\bar{\mathbf{H}}^H\bar{\mathbf{H}}))$, where $\bar{\mathbf{H}} = [\boldsymbol{H}^H, \mathbf{0}_{N\times(M-K)}]^H$, which is then normalized to obtain $\boldsymbol{x}_{\text{norm}} = \frac{\boldsymbol{x}}{\max(\boldsymbol{x})}$. Then $\boldsymbol{x}_{\text{norm}}$ is used as the input of the trained DNN to output the prediction vector $\hat{\boldsymbol{b}}$. It is worth noting that the DNN does not provide absolute prediction, e.g., 0 or 1, but probabilistic uncertainties, e.g., $-1 \le \hat{b}[n] \le 1, \forall n$. In general, the larger an element in $\hat{\boldsymbol{b}}$ is, the higher chance this element is the best antenna subset. Consequently, the subset $\mathcal{A}_{n^\star}$ corresponding to the largest output prediction, i.e., $n^\star = \arg\max_n \hat{b}[n]$, can be selected. However, the prediction is not always precise. Therefore, in order to improve the performance of the L-ASPD algorithm, instead of choosing only one best candidate, we select K_S subsets, denoted by $\boldsymbol{\mathcal{K}}_S$, corresponding to the K_S largest elements in $\hat{\boldsymbol{b}}$. Then, we apply the precoding design (Algorithm 1 or 2) on these K_S subsets. Intuitively, larger values of K_S will increase the chance for the L-ASPD algorithm to select the best antenna subset at an expense of more computation complexity. The steps of the L-ASPD algorithm are listed in Algorithm 4. Compared with the JASPD algorithm, the L-ASPD algorithm significantly reduces the computational time since it tests only K_S promising candidates instead of $\binom{N}{M}$. Consequently, the L-ASPD algorithm is expected to achieve a better effective sum rate than that of the JASPD algorithm, especially when $K_S \ll \binom{N}{M}$.

V. PERFORMANCE EVALUATION

In this section, we evaluate the performance of the proposed algorithms via numerical results. The users are uniformly distributed in an area between 50 and 300 meters from the BS. We employ the WINNER II line-of-sight pathloss model [33], which results in a pathloss that is uniformly distributed between -59.4 dB and -74.6 dB. All wireless channels are subject to Rayleigh fading. The channel bandwidth $B = 1$ MHz and the noise spectral density is -140 dBm/Hz. We adopt the LTE specifications [34] that one c.u. lasts one symbol duration and is equal to 66.7 μs, and one block duration comprises 200 c.u.. The BS is assumed to spend 0.2 c.u.

TABLE II
SIMULATION PARAMETERS

Parameters	Value
Cell radius	300 m
BS's transmit power	1 W - 5W
Number of RF chains M	4
Number of antennas N	Varies
Number of users K	Varies between 1 and M
QoS $\eta_k = \eta, \forall k$	2 Mbps
Training method	Scaled conjugate gradient
Activation function (hidden layers)	`tansig`
Activation function (output layer)	$\texttt{soft} - \texttt{max}$
Loss function	Cross-entropy

to solve one convex optimization problem [36]. As a result, it takes $0.2K_S$ c.u. to execute the proposed L-ASPD algorithm, where K_S is the number of predicted subsets. We employ an DNN with two hidden layers to train the learning model for the L-ASPD algorithm, each layer consists of 100 nodes.[5] SVM can also be employed for its fast training phase, however, it results in poorer performance compared to DNN. This is because SVM results in hyperplanes to discriminate the data whereas the DNN can discriminate data using more elaborate functions. The DNN is trained using the scaled conjugate gradient method. Other simulation parameters are listed in Table II.

A. Convergence of the Proposed Optimization Algorithms

We first evaluate the convergence performance of the proposed iterative Algorithm 1 and 2 presented in Section III. The results are obtained from 200 random realizations of channel fading coefficients and users' locations. For each realization, we run both Algorithm 1 and 2 until they converge. Fig. 4a compares the sum-rate obtained by the two proposed algorithms as a function of the iteration number. It is clearly shown that both algorithms converge quickly after less than 10 iterations, which demonstrates the effectiveness of the proposed iterative algorithms.

In order to provide insights on the computation performance of the proposed algorithms, we show in Fig 4b the sum-rate versus the simulation time. Both algorithms are carried out by SeDuMi solver integrated in Matlab 2017b, running on a personal laptop with the Intel i7-6820HQ CPU and 8GB RAM. It is observed that Algorithm 2 executes slightly faster than Algorithm 1, however, achieves a smaller sum-rate. The performance gain brought by Algorithm 1 results from the fact that it uses more memory than Algorithm 2, as shown in Table III. Due to superior performance, we will employ the proposed Algorithm 1 in the remaining results.

B. Performance-Complexity Trade-Off of the L-ASPD

In this subsection, we examine the efficiency of the proposed L-ASPD algorithm via a performance-complexity gain trade-off. By confining the search space of the prediction output, i.e., $K_{\mathcal{S}}$ - the number of potential antenna subsets, we can manage the complexity of the L-ASPD algorithm since it works only on $K_{\mathcal{S}}$ candidates. The complexity gain of

[5]We heuristically try a different number of hidden layers and find out that a DNN with two hidden layers is sufficient for our problem.

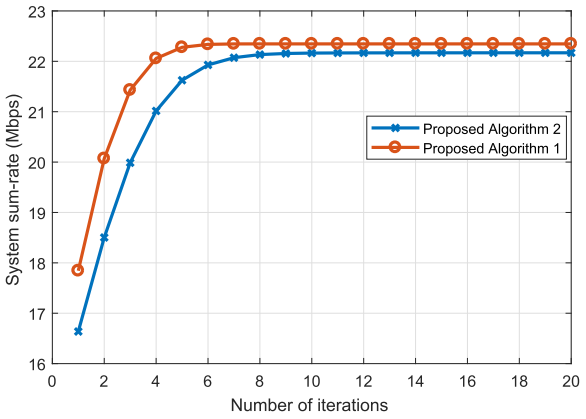

(a) Sum rate versus number of iterations

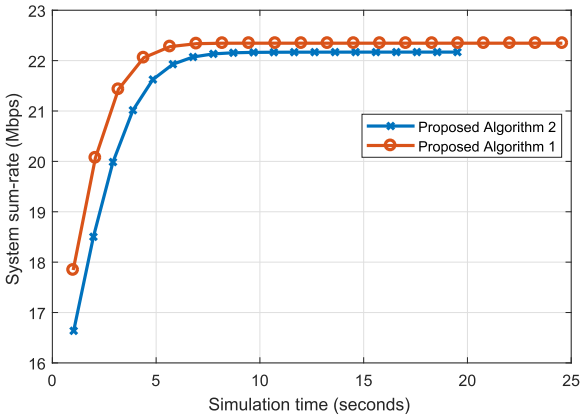

(b) Sum rate versus simulation time

Fig. 4. Performance comparison of the proposed Algorithm 1 and 2, $P_{tot} = 37$ dBm and $K = 4$. Both algorithms converge in less than 10 iterations.

TABLE III
NUMBER OF VARIABLES REQUIRED BY ALGORITHM 1 AND 2 FOR DIFFERENT SETUPS FOR $N = 8$

M	2	3	4	5
Algorithm 1	267	400	533	666
Algorithm 2	55	94	141	196

the L-ASPD algorithm is defined as the relative time saving compared to the exhaustive search that tests every antenna subsets, which is calculated as:

$$\theta(K_{\mathcal{S}}) = \frac{\tau(\binom{N}{M} - K_{\mathcal{S}})}{\tau\binom{N}{M}} = 1 - \frac{K_{\mathcal{S}}}{\binom{N}{M}}, \tag{17}$$

where τ is the computational time spent on the optimization of the precoding vectors for a selected antenna subset. The performance gain is defined as the ratio between the sum rate obtained by the L-ASPD algorithm divided by the optimal sum rate which is achieved by searching all possible antenna subsets.

Fig. 5 plots the performance-complexity tradeoff of the proposed L-ASPD algorithm with $M = 4$ RF chains and $N = 8$ total number of antennas. It is observed that the L-ASPD algorithm retains more than 96% of the optimal sum rate (which is obtained by exhaustive search) while saving more than 95% complexity. Even when spending only 2%

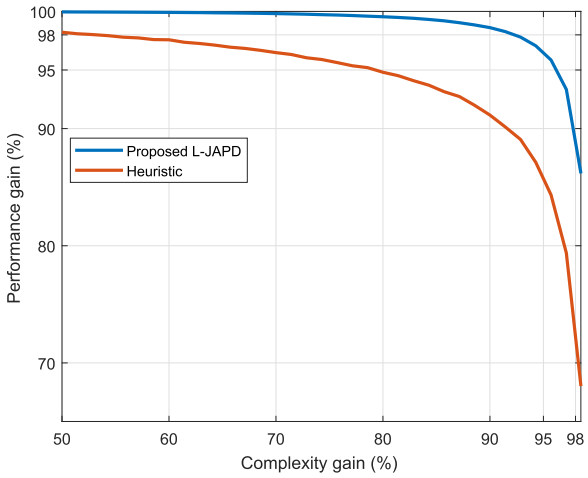

Fig. 5. Performance-complexity tradeoff of the proposed L-ASPD. $M = 4$, $N = 8$.

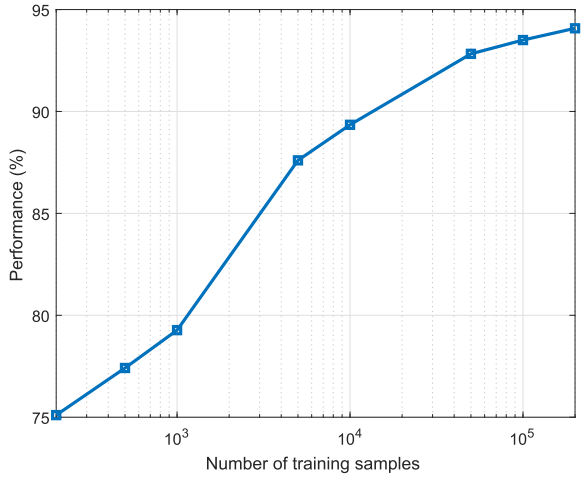

Fig. 6. Learning (relative) performance versus the number of training samples. $M = 4, N = 8$.

the computational time, the L-ASPD algorithm still achieves 86% of the optimal performance, which confirms the effectiveness of the proposed L-ASPD algorithm. Compared with the heuristic solution, the L-ASPD algorithm further reduces more than 13% the computational time at the 95% performance gain target.

Fig. 6 plots the relative performance in the real-time prediction of the L-ASPD algorithm versus the number of training samples. The relative performance is measured as the ratio of the sum rate of the L-ASPD algorithm divided by the one obtained by the JASPD algorithm. Each training sample is generated randomly and captures the randomness in both channel small-scale fading and user location. In general, having more training samples results in better prediction accuracy since the L-ASPD algorithm learns more about the intrinsic relation between the selected antennas and the input features. It is shown that 2×10^5 training samples are sufficient for the L-ASPD algorithm to achieve more than 94% of the optimal performance.

C. Online Performance Comparison

This subsection demonstrates the effectiveness of the proposed L-ASPD algorithm via performance comparisons with

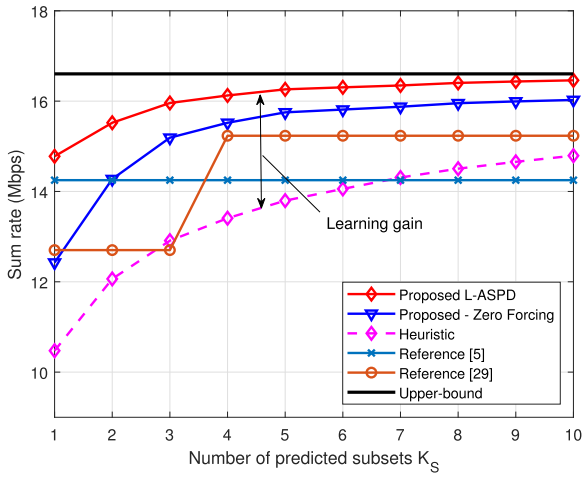

Fig. 7. Sum rate performance of the proposed algorithms versus the number of predicted subsets K_S. $P_{tot} = 33$ dBm, $M = 4$ and $N = 8$.

existing solutions in difference scenarios. The first baseline scheme is proposed in [5], which employs block diagonalization to consecutively eliminate antennas that incur the largest transmit power cost. The second baseline is introduced in [29], which is a learning-assisted antenna selection for multicasting. In addition, a *Heuristic* search is also presented, which applies the proposed beamforming design but it searches for the antenna subset heuristically. We note that the comparison with [27], [28], [30] is not applicable because [27], [28] consider a single-user system and [30] selects only a single antenna.

Fig. 7 shows the achievable sum rate as a function of K_S - the most promising subsets predicted by the proposed L-ASPD algorithm. In order to reveal the benefit of proposed beamforming design in Algorithm 1, we also show a curve, which applies a zero-forcing based power control [35] on the antenna subsets predicted by Algorithm 4. This curve is named as *Proposed - Zero Forcing* in the figures. It is shown that the proposed L-ASPD algorithm significantly outperforms all schemes for all observed K_S values. In general, having more predicted subsets K_S results in a larger sum rate, which is in line with the results in Fig. 5. In particular, by searching over the most five promising subsets, the proposed L-ASPD algorithm achieves 1 Mbps and 2 Mbps higher than schemes in [29] and [5], respectively. We note that the sum rate of the scheme in [5] is independent from K_S since it predicts the best antenna subset. Similarly, the performance curve of [29] has a step-shape because it uses the active antennas as the prediction outputs, hence it is only able to confine the original search space to $\binom{M+n}{M}$ subsets, with $0 \leq n \leq N - M$.

Fig. 8 plots the sum rate as a function of the transmit power. The effectiveness of the proposed learning-based method is shown via the largest sum rate achieved by the L-JAPD algorithm compared to other schemes. On average, the L-JAPD algorithm produces 1.5 Mbps and 2 Mbps more than the solution in [29] and heuristic scheme, respectively, proving that the DNN has been well trained. Compared to the solution in [5], the L-ASPD algorithm achieves a relative sum rate gain of 5 Mbps and 2 Mbps at the transmit power equal to 30 dBm and 33 dBm, respectively. One interesting observation is that

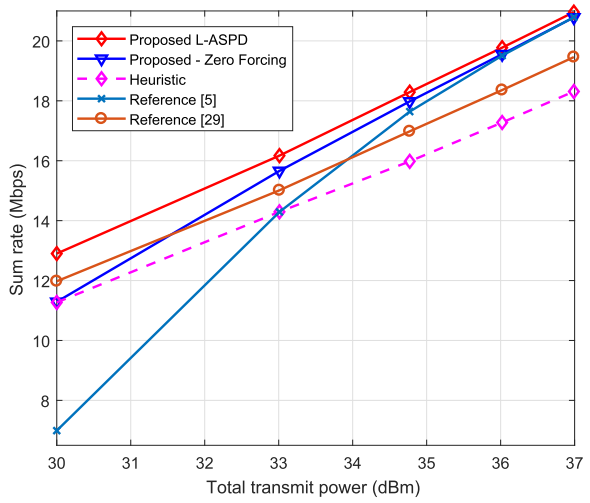

Fig. 8. Sume rate performance of the proposed algorithms versus the total transmit power P_{tot}. $K_S = 7$ and $N = 8$ available antennas.

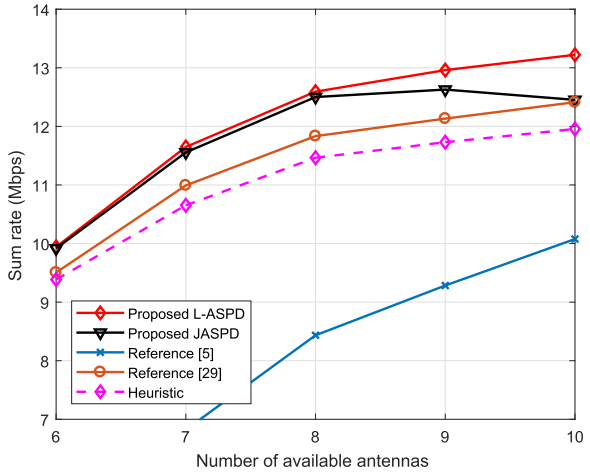

Fig. 9. Effective sum rate comparison for various number of total antennas N. $P_{tot} = 30$ dBm, $M = 4, K_S = 10$.

the Zero-forcing scheme and the solution in [5] approach the performance of the L-ASPD algorithm when the total transmit power budget increases. This is because for large P_{tot}, the BS has sufficient power budget to fully mitigate inter-user interference. For small P_{tot}, the system resource becomes scarce, therefore completely eliminating inter-user interference is far from the optimum, which is shown in a big gap between the L-ASPD algorithm and these two schemes. In such high-load scenarios, employing the proposed design is highly beneficial.

Fig. 9 presents the effective sum rate for different total antennas numbers N. For a fair comparison, the total transmit power is kept constant at 30 dBm and the total overhead of channel estimation and computation is taken into account. For the former, it takes 8 c.u. to obtain the CSI when the total antenna number is $6, 7, 8$, and takes 12 c.u. when the number of antennas is 9 and 10. Consider the latter, the L-ASPD algorithm only searches over 10 most promising candidates, while the JASPD algorithm tries all $\binom{N}{M}$ antenna subsets. In general, having more antennas results in a better effective sum rate of all schemes, which confirms the benefit of antenna selection. Interestingly, the proposed L-ASPD algorithm achieves the best performance and outperforms the exhaustive search scheme, especially for large N, which is in contrast to common understanding that the exhaustive search achieves the best performance. This is because we take the computation time into account in the comparison, as shown in (2). As a result, the exhaustive search scheme spends too much time in searching for the best subset, particularly with large N, resulting in smaller effective rates. As an example for $N = 10$, the exhaustive search scheme requires a computation time which is 21 times more than that of the L-ASPD algorithm.

VI. Conclusion

We studied the joint design for antenna selection and precoding vectors in multi-user multi-antenna systems to fully exploit the spatial diversity. We first proposed a (near) optimal joint antenna selection and precoding algorithm to maximize the system sum rate, subjected to the users' QoS and limited transmit power. The proposed joint design successively optimizes the precoding vectors via two proposed iterative optimization algorithms based on the semidefinite relaxation and successive convex approximation methods. In order to further improve the optimization efficiency, we then developed a machine learning-based solution to provide appropriate and time-stringent antenna predictions. The proposed learning-based algorithm is robust against the number of users and their locations, the BS's transmit power, as well as the channel fading. We showed via simulation results that the proposed learning-based solution significantly outperforms existing selection schemes and the exhaustive search-based solution.

Based on the outcome of this work, several research directions can be considered. The first problem is how to improve the training phase efficiency, which is especially important when the number of available antennas is very large. In such a case, a low-complexity precoding design, e.g., zero-forcing, can be used to quickly obtain sufficient training samples. The second problem lies in dealing with the network dynamics, which requires the learning model to frequently and timely adapted. Transfer leaning and reinforcement learning are promising solutions in this case to avoid retraining the whole network.

Appendix A
Proof of Proposition 1

Denote $\left(\boldsymbol{W}_\star^{(t)}, \boldsymbol{x}_\star^{(t)}, \boldsymbol{y}_\star^{(t)}\right)$ as the optimal solution of P2$(\boldsymbol{y}_0^{(t)})$ at iteration t. We will show that if $y_{\star k}^{(t)} < y_{0k}^{(t)}, \forall k$, then by using $y_{0k}^{(t+1)} = y_{\star k}^{(t)}$ in the $(t+1)$-th iteration, we will have $\sum_k x_{\star k}^{(t+1)} > \sum_k x_{\star k}^{(t)}$, where $\{x_{\star k}^{(t+1)}\}_{k=1}^K$ is the solution at iteration $t+1$. Indeed, by choosing a relatively large initial value $\boldsymbol{y}_0^{(1)}$, we always have $y_{\star k}^{(1)} < y_{0k}^{(1)}, \forall k$.

Denote $f(y; a) = e^a(y - a + 1)$ as the first order approximation of the e^y function at a. At iteration $t+1$, we have $y_{0k}^{(t+1)} = y_{\star k}^{(t)}, \forall k$. Therefore, $f(y; y_{\star k}^{(t)})$ is used in the right-hand side of constraint (9a) at the $(t+1)$-th iteration. Consider a candidate $(y_1^{(t+1)}, \ldots, y_K^{(t+1)})$ for any $y_k^{(t+1)} \in (\hat{y}_k, y_{\star k}^{(t)})$, where $\hat{y}_k = y_{\star k}^{(t)} - 1 + e^{y_{0k}^{(t)} - y_{\star k}^{(t)}}(y_{\star k}^{(t)} - y_{0k}^{(t)} + 1)$. Because function exp()

is convex and $y_k^{(t+1)} < y_{\star k}^{(t)}$, then we have $f(y_k^{(t+1)}; y_{\star k}^{(t)}) > f(y_{\star k}^{(t)}; y_{0k}^{(t)}), \forall k$. Therefore, there exits $\boldsymbol{W}_k^{(t+1)}$ and $x_k^{(t+1)} > x_{\star k}^{(t)}$ which satisfies constraints (7) and (9a). Consider a new set $\{\boldsymbol{W}_k^{(t+1)}, x_k^{(t+1)}, y_k^{(t+1)}\}_{k=1}^K$. This set satisfies all the constraints of problem P2($\boldsymbol{y}_\star^{(t)}$), and therefore is a feasible solution of the optimization problem. As the result, the optimal objective at iteration $(t+1)$, $\frac{\bar{B}}{\log(2)} \sum_k x_{\star k}^{(t+1)}$, must satisfy $\frac{\bar{B}}{\log(2)} \sum_k x_{\star k}^{(t+1)} \geq \frac{\bar{B}}{\log(2)} \sum_k x_k^{(t+1)} > \frac{\bar{B}}{\log(2)} \sum_k x_{\star k}^{(t)}$, which completes the proof of Proposition 1.

Appendix B
Convexity of Function $\frac{\boldsymbol{x}^T \boldsymbol{A} \boldsymbol{x}}{y}$

To prove the convexity of $F(\boldsymbol{x}, y) = \frac{\boldsymbol{x}^T \boldsymbol{A} \boldsymbol{x}}{y}$ for any positive semi-definite matrix $\boldsymbol{A}$, we need to show that the Hessian matrix of $F(\boldsymbol{x}, y)$ is positive semidefinite. Indeed, the Hessian matrix of $F(\boldsymbol{x}, y)$ is

$$\boldsymbol{H}_F = \begin{bmatrix} \dfrac{\boldsymbol{A}+\boldsymbol{A}^T}{y} & -\dfrac{(\boldsymbol{A}+\boldsymbol{A}^T)\boldsymbol{x}}{y^2} \\ -\dfrac{\boldsymbol{x}^T(\boldsymbol{A}+\boldsymbol{A}^T)}{y^2} & \dfrac{2\boldsymbol{x}^T\boldsymbol{A}\boldsymbol{x}}{y^3} \end{bmatrix}.$$

For arbitrary vector $\boldsymbol{c} = [\boldsymbol{a}^T b]^T$, where $\boldsymbol{a} \in \mathbb{R}^{N\times 1}$, consider a function

$$\begin{aligned} &\boldsymbol{c}^T \boldsymbol{H}_F \boldsymbol{c} \\ &= \frac{\boldsymbol{a}^T(\boldsymbol{A}+\boldsymbol{A}^T)\boldsymbol{a}}{y} - \frac{\boldsymbol{a}^T(\boldsymbol{A}+\boldsymbol{A}^T)\boldsymbol{x}b}{y^2} \\ &\quad - \frac{\boldsymbol{x}^T(\boldsymbol{A}+\boldsymbol{A}^T)\boldsymbol{a}b}{y^2} + \frac{2\boldsymbol{x}^T\boldsymbol{A}\boldsymbol{x}b^2}{y^3} \\ &\overset{(*)}{=} \frac{\boldsymbol{a}^T(\boldsymbol{A}+\boldsymbol{A}^T)\boldsymbol{a}}{y} - 2\frac{\boldsymbol{a}^T(\boldsymbol{A}+\boldsymbol{A}^T)\boldsymbol{x}b}{y^2} + \frac{\boldsymbol{x}^T(\boldsymbol{A}+\boldsymbol{A}^T)\boldsymbol{x}b^2}{y^3} \\ &= \frac{\boldsymbol{a}^T\tilde{\boldsymbol{A}}\boldsymbol{a} - 2\boldsymbol{a}^T\tilde{\boldsymbol{A}}\tilde{\boldsymbol{x}} + \tilde{\boldsymbol{x}}^T\tilde{\boldsymbol{A}}\tilde{\boldsymbol{x}}}{y}, \end{aligned} \tag{18}$$

where $\tilde{\boldsymbol{A}} \triangleq \boldsymbol{A}^T + \boldsymbol{A}$, $\tilde{\boldsymbol{x}} \triangleq \boldsymbol{x}b/y$ and $(*)$ results from the fact that $\boldsymbol{A}$ is symmetric and $\boldsymbol{a}^T\tilde{\boldsymbol{A}}\tilde{\boldsymbol{x}} = \tilde{\boldsymbol{x}}^T\tilde{\boldsymbol{A}}\boldsymbol{a}$. It is obvious that the RHS of (18) is always non-negative for $y > 0$ and positive semi-definite matrix $\tilde{\boldsymbol{A}}$, which concludes the positive semi-definite of the Hessian matrix of $F(\boldsymbol{x}, y)$.

References

[1] E. G. Larsson, O. Edfors, F. Tufvesson, and T. L. Marzetta, "Massive MIMO for next generation wireless systems," *IEEE Commun. Mag.*, vol. 52, no. 2, pp. 186–195, Feb. 2014.

[2] R. W. Heath, Jr., and A. Paulraj, "Antenna selection for spatial multiplexing systems based on minimum error rate," in *Proc. IEEE Int. Conf. Commun.*, Jun. 2001, pp. 2276–2280.

[3] Y. Pei, T.-H. Pham, and Y.-C. Liang, "How many RF chains are optimal for large-scale MIMO systems when circuit power is considered?" in *Proc. IEEE Global Commun. Conf.*, Dec. 2012, pp. 3868–3873.

[4] J. G. Andrews *et al.*, "What will 5G be?" *IEEE J. Sel. Areas Commun.*, vol. 32, no. 6, pp. 1065–1082, Jun. 2014.

[5] R. Chen, J. G. Andrews, and R. W. Heath, Jr., "Efficient transmit antenna selection for multiuser MIMO systems with block diagonalization," in *Proc. IEEE GLOBECOM IEEE Global Telecommun. Conf.*, Nov. 2007, pp. 3499–3503.

[6] O. Mehanna, N. D. Sidiropoulos, and G. B. Giannakis, "Joint multicast beamforming and antenna selection," *IEEE Trans. Signal Process.*, vol. 61, no. 10, pp. 2660–2674, May 2013.

[7] S. Qin, G. Li, G. Lv, G. Zhang, and H. Hui, "L1/2-regularization based antenna selection for RF-chain limited massive MIMO systems," in *Proc. IEEE 84th Veh. Technol. Conf. (VTC-Fall)*, Sep. 2016, pp. 1–5.

[8] T. X. Vu, S. Chatzinotas, S. ShahbazPanahi, and B. Ottersten, "Joint power allocation and access point selection for cell-free massive MIMO," in *Proc. IEEE Int. Conf. Commun. (ICC)*, Jun. 2020, pp. 1–6.

[9] M. S. Ibrahim, A. Konar, M. Hong, and N. D. Sidiropoulos, "Mirror-prox SCA algorithm for multicast beamforming and antenna selection," in *Proc. IEEE 19th Int. Workshop Signal Process. Adv. Wireless Commun.*, Jun. 2018, pp. 1–5.

[10] O. Tervo, L.-N. Tran, H. Pennanen, S. Chatzinotas, B. Ottersten, and M. Juntti, "Energy-efficient multicell multigroup multicasting with joint beamforming and antenna selection," *IEEE Trans. Signal Process.*, vol. 66, no. 18, pp. 4904–4919, Sep. 2018.

[11] S. He, Y. Huang, J. Wang, L. Yang, and W. Hong, "Joint antenna selection and energy-efficient beamforming design," *IEEE Signal Process. Lett.*, vol. 23, no. 9, pp. 1165–1169, Sep. 2016.

[12] T. O'Shea and J. Hoydis, "An introduction to deep learning for the physical layer," *IEEE Trans. Cognit. Commun. Netw.*, vol. 3, no. 4, pp. 563–575, Dec. 2017.

[13] A. Zappone, M. Di Renzo, and M. Debbah, "Wireless networks design in the era of deep learning: Model-based, AI-based, or both?" *IEEE Trans. Commun.*, vol. 67, no. 10, pp. 7331–7376, Oct. 2019.

[14] A. Zappone, M. Di Renzo, M. Debbah, T. T. Lam, and X. Qian, "Model-aided wireless artificial intelligence: Embedding expert knowledge in deep neural networks for wireless system optimization," *IEEE Veh. Technol. Mag.*, vol. 14, no. 3, pp. 60–69, Sep. 2019.

[15] L. Lei, L. You, G. Dai, T. X. Vu, D. Yuan, and S. Chatzinotas, "A deep learning approach for optimizing content delivering in cache-enabled HetNet," in *Proc. IEEE Int. Symp. Wireless Commun. Syst.*, Aug. 2017, pp. 449–453.

[16] W. Xia, G. Zheng, Y. Zhu, J. Zhang, J. Wang, and A. P. Petropulu, "A deep learning framework for optimization of MISO downlink beamforming," *IEEE Trans. Commun.*, vol. 68, no. 3, pp. 1866–1880, Mar. 2020.

[17] H. Huang, W. Xia, J. Xiong, J. Yang, G. Zheng, and X. Zhu, "Unsupervised learning-based fast beamforming design for downlink MIMO," *IEEE Access*, vol. 7, pp. 7599–7605, 2019.

[18] H. Huang, Y. Peng, J. Yang, W. Xia, and G. Gui, "Fast beamforming design via deep learning," *IEEE Trans. Veh. Technol.*, vol. 69, no. 1, pp. 1065–1069, Jan. 2020.

[19] J. Jang, H. Lee, S. Hwang, H. Ren, and I. Lee, "Deep learning-based limited feedback designs for MIMO systems," *IEEE Wireless Commun. Lett.*, vol. 9, no. 4, pp. 558–561, Apr. 2020.

[20] T. Lin and Y. Zhu, "Beamforming design for large-scale antenna arrays using deep learning," *IEEE Wireless Commun. Lett.*, vol. 9, no. 1, pp. 103–107, Jan. 2020.

[21] T. E. Bogale, X. Wang, and L. B. Le, "Adaptive channel prediction, beamforming and scheduling design for 5G V2I network: Analytical and machine learning approaches," *IEEE Trans. Veh. Technol.*, vol. 69, no. 5, pp. 5055–5067, May 2020.

[22] R. Shafin *et al.*, "Self-tuning sectorization: Deep reinforcement learning meets broadcast beam optimization," *IEEE Trans. Wireless Commun.*, vol. 19, no. 6, pp. 4038–4053, Jun. 2020.

[23] F. B. Mismar, B. L. Evans, and A. Alkhateeb, "Deep reinforcement learning for 5G networks: Joint beamforming, power control, and interference coordination," *IEEE Trans. Commun.*, vol. 68, no. 3, pp. 1581–1592, Mar. 2020.

[24] A. Alkhateeb, "DeepMIMO: A generic deep learning dataset for millimeter wave and massive MIMO applications," in *Proc. Info. Theory Appl. Workshop (ITA)*, San Diego, CA, USA, Feb. 2019, pp. 1–8.

[25] H. Sun, X. Chen, Q. Shi, M. Hong, X. Fu, and N. D. Sidiropoulos, "Learning to optimize: Training deep neural networks for wireless resource management," in *Proc. IEEE Int. Workshop Signal Process. Adv. Wireless Commun.*, Jul. 2017, p. 247—-252.

[26] L. Lei, T. X. Vu, L. You, S. Fowler, and D. Yuan, "Efficient minimum-energy scheduling with machine-learning based predictions for multiuser MISO systems," in *Proc. IEEE Int. Conf. Commun.*, May 2018, pp. 1–6.

[27] A. M. Elbir and K. V. Mishra, "Joint antenna selection and hybrid beamformer design using unquantized and quantized deep learning networks," *IEEE Trans. Wireless Commun.*, vol. 19, no. 3, pp. 1677–1688, Mar. 2020.

[28] J. Joung, "Machine learning-based antenna selection in wireless communications," *IEEE Commun. Lett.*, vol. 20, no. 11, pp. 2241–2244, Nov. 2016.

[29] M. S. Ibrahim, A. S. Zamzam, X. Fu, and N. D. Sidiropoulos, "Learning-based antenna selection for multicasting," in *Proc. IEEE 19th Int. Workshop Signal Process. Adv. Wireless Commun.*, Jun. 2018, pp. 1–5.
[30] D. He, C. Liu, T. Q. S. Quek, and H. Wang, "Transmit antenna selection in MIMO wiretap channels: A machine learning approach," *IEEE Wireless Commun. Lett.*, vol. 7, no. 4, pp. 634–637, Aug. 2018.
[31] T. X. Vu, L. Lei, S. Chatzinotas, and B. Ottersten, "Machine learning based antenna selection and power allocation in multi-user MISO systems," in *Proc. Int. Symp. Modeling Optim. Mobile, Ad Hoc, Wireless Netw.*, Jun. 2019, pp. 1–6.
[32] Z.-Q. Luo, W.-K. Ma, A. So, Y. Ye, and S. Zhang, "Semidefinite relaxation of quadratic optimization problems," *IEEE Signal Process. Mag.*, vol. 27, no. 3, pp. 20–34, May 2010.
[33] P. Kyosti *et al.*, "WINNER II channel models," White Paper D1.1.2 V1.2, 2007.
[34] Telesystem Innovations, "LTE in a nutshell: The physical layer," White Paper, 2010.
[35] T. X. Vu, L. Lei, S. Vuppala, A. Kalantari, S. Chatzinotas, and B. Ottersten, "Latency minimization for content delivery networks with wireless edge caching," in *Proc. IEEE Int. Conf. Commun.*, Kansas City, MO, USA, May 2018, pp. 1–6.
[36] J. Mattingley and S. Boyd, "Real-time convex optimization in signal processing," *IEEE Signal Process. Mag.*, vol. 27, no. 3, pp. 50–61, May 2010.

Thang X. Vu (Member, IEEE) received the B.S. and M.Sc. degrees in electronics and telecommunications engineering from the VNU University of Engineering and Technology, Vietnam, in 2007 and 2009, respectively, and the Ph.D. degree in electrical engineering from Paris-Sud University, France, in 2014. From September 2010 to May 2014, he was with the Laboratory of Signals and Systems (LSS), a joint laboratory of CNRS, CentraleSupelec and University Paris-Sud XI, France. From July 2014 to January 2016, he was a Post-Doctoral Researcher with the Information Systems Technology and Design (ISTD) Pillar, Singapore University of Technology and Design (SUTD), Singapore. He is currently a Research Scientist with the Interdisciplinary Centre for Security, Reliability and Trust (SnT), University of Luxembourg. His research interests include wireless communications, with particular interests of wireless edge caching, cloud radio access networks, machine learning for communications, and cross-layer resources optimization. In 2010, he received the Allocation de Recherche Fellowship to study the Ph.D. degree in France. He was a recipient of the SigTelCom 2019 Best Paper Award.

Symeon Chatzinotas (Senior Member, IEEE) received the M.Eng. degree in telecommunications from the Aristotle University of Thessaloniki, Thessaloniki, Greece, in 2003, and the M.Sc. and Ph.D. degrees in electronic engineering from the University of Surrey, Surrey, U.K., in 2006 and 2009, respectively. He was a Visiting Professor with the University of Parma, Italy. He was involved in numerous research and development projects of the National Center for Scientific Research Demokritos, the Center of Research and Technology Hellas, and the Center of Communication Systems Research, University of Surrey. He is currently a Full Professor/Chief Scientist I and the Co-Head of the SIGCOM Research Group at SnT, University of Luxembourg. He has coauthored more than 400 technical articles in refereed international journals, conferences, and scientific books. He was a co-recipient of the 2014 IEEE Distinguished Contributions to Satellite Communications Award, the CROWNCOM 2015 Best Paper Award, and the 2018 EURASIC JWCN Best Paper Award. He is also the editorial board of the IEEE OPEN JOURNAL OF VEHICULAR TECHNOLOGY and the *International Journal of Satellite Communications and Networking*.

Van-Dinh Nguyen (Member, IEEE) received the B.E. degree in electrical engineering from the Ho Chi Minh City University of Technology, Vietnam, in 2012, and the M.E. and Ph.D. degrees in electronic engineering from Soongsil University, Seoul, South Korea, in 2015 and 2018, respectively.

He was a Post-Doctoral Researcher and a Lecturer with Soongsil University, a Post-Doctoral Visiting Scholar with the University of Technology Sydney, Australia, from July 2018 to August 2018, and a Ph.D. Visiting Scholar with Queen's University Belfast, U.K., from June 2015 to July 2015 and in August 2016. He is currently a Research Associate with the Interdisciplinary Centre for Security, Reliability and Trust (SnT), University of Luxembourg. His current research interests include fog/edge computing, the Internet of Things, 5G networks, and machine learning for wireless communications. He received several best conference paper awards, IEEE TRANSACTIONS ON COMMUNICATIONS Exemplary Reviewer 2018, and IEEE GLOBECOM Student Travel Grant Award 2017. He has authored or coauthored 40 papers published in international journals and conference proceedings. He has served as a reviewer for many top-tier international journals on wireless communications, and has also been a technical programme committee member for several flag-ship international conferences in the related fields. He is an Editor of the IEEE OPEN JOURNAL OF THE COMMUNICATIONS SOCIETY and IEEE COMMUNICATIONS LETTERS.

Dinh Thai Hoang (Member, IEEE) received the Ph.D. degree in computer science and engineering from Nanyang Technological University, Singapore, in 2016. He is currently a Faculty Member of the School of Electrical and Data Engineering, University of Technology Sydney, Australia. His research interests include emerging topics in wireless communications and networking, such as machine learning, ambient backscatter communications, IRS, mobile edge intelligence, cybersecurity, the Internet of Things (IoT), and 5G/6G networks. He has received several awards, including the Australian Research Council. He is an Editor of IEEE WIRELESS COMMUNICATIONS LETTERS and IEEE TRANSACTIONS ON COGNITIVE COMMUNICATIONS AND NETWORKING.

Diep N. Nguyen (Senior Member, IEEE) received the M.E. degree in electrical and computer engineering from the University of California at San Diego (UCSD) and the Ph.D. degree in electrical and computer engineering from The University of Arizona (UA). He is a Faculty Member of the Faculty of Engineering and Information Technology, University of Technology Sydney (UTS). Before joining the UTS, he was a DECRA Research Fellow at Macquarie University, and a member of Technical Staff at Broadcom, CA, USA, and ARCON Corporation, Boston, consulting the Federal Administration of Aviation on turning detection of UAVs and aircraft, U.S. Air Force Research Lab on anti-jamming. His current research interests include computer networking, wireless communications, and machine learning applications, with an emphasis on systems performance and security/privacy. He has received several awards from LG Electronics, UCSD, UA, U.S. National Science Foundation, and Australian Research Council. He is an Editor or Associate Editor of the IEEE TRANSACTIONS ON MOBILE COMPUTING, IEEE ACCESS, IEEE SENSORS JOURNAL, and IEEE OPEN JOURNAL OF THE COMMUNICATIONS SOCIETY (OJ-COMS).

Marco Di Renzo (Fellow, IEEE) received the Laurea *(cum laude)* and Ph.D. degrees in electrical engineering from the University of L'Aquila, Italy, in 2003 and 2007, respectively, and the Habilitation a Diriger des Recherches (Doctor of Science) degree from Paris-Sud University, France, in 2013.

Since 2010, he has been with the French National Center for Scientific Research (CNRS), where he is currently the CNRS Research Director (CNRS Professor) with the Laboratory of Signals and Systems (L2S), Paris-Saclay University—CNRS, and CentraleSupelec, Paris, France. In Paris-Saclay University, he serves as the Coordinator for the Communications and Networks Research Area with the Laboratory of Excellence DigiCosme, and as a member of the Admission and Evaluation Committee of the Ph.D. School on Information and Communication Technologies. He is a fellow of IET. He has received several individual distinctions and research awards, which include the IEEE Communications Society Best Young Researcher Award for Europe, Middle East and Africa, the Royal Academy of Engineering Distinguished Visiting Fellowship, the IEEE Jack Neubauer Memorial Best System Paper Award, the IEEE Communications Society Young Professional in Academia Award, the SEE-IEEE Alain Glavieux Award, and a 2019 IEEE ICC Best Paper Award. In 2019, he was a recipient of a Nokia Foundation Visiting Professorship for conducting research on metamaterial-assisted wireless communications with Aalto University, Finland. He is also a Highly Cited Researcher (Clarivate Analytics, Web of Science), a World's Top 2% Scientist from Stanford University. He also serves as the Founding Chair of the Special Interest Group on Reconfigurable Intelligent Surfaces of the Wireless Technical Committee of the IEEE Communications Society. He also serves as the Editor-in-Chief of IEEE COMMUNICATIONS LETTERS and a Distinguished Speaker of the IEEE Vehicular Technology Society. From 2017 to 2020, he was a Distinguished Lecturer of the IEEE Vehicular Technology Society and IEEE Communications Society. He served as an Editor and the Associate Editor-in-Chief of IEEE COMMUNICATIONS LETTERS, and an Editor of IEEE TRANSACTIONS ON COMMUNICATIONS and IEEE TRANSACTIONS ON WIRELESS COMMUNICATIONS. He is also the Founding Lead Editor of the IEEE Communications Society Best Readings in Reconfigurable Intelligent Surfaces.

Björn Ottersten (Fellow, IEEE) received the M.S. degree in electrical engineering and applied physics from Linköping University, Linköping, Sweden, in 1986, and the Ph.D. degree in electrical engineering from Stanford University, Stanford, CA, USA, in 1990.

He has held research positions with the Department of Electrical Engineering, Linköping University; the Information Systems Laboratory, Stanford University; Katholieke Universiteit Leuven, Leuven, Belgium; and the University of Luxembourg, Luxembourg. From 1996 to 1997, he was the Director of Research with ArrayComm, Inc., a start-up in San Jose, CA, USA, based on his patented technology. In 1991, he was an appointed Professor of Signal Processing with the KTH Royal Institute of Technology, Stockholm, Sweden, where he has been the Head of the Department for Signals, Sensors, and Systems and the Dean of the School of Electrical Engineering. He is currently the Director of the Interdisciplinary Centre for Security, Reliability and Trust, University of Luxembourg. He is a fellow of EURASIP. He was a recipient of the IEEE Signal Processing Society Technical Achievement Award, the EURASIP Group Technical Achievement Award, and the European Research Council advanced research grant twice. He has coauthored journal articles that received the IEEE Signal Processing Society Best Paper Award in 1993, 2001, 2006, 2013, and 2019, and eight IEEE conference papers best paper awards. He has been a Board Member of IEEE Signal Processing Society and the Swedish Research Council, and currently serves on the boards of EURASIP and the Swedish Foundation for Strategic Research. He has served as the Editor-in-Chief of *EURASIP Journal on Advances in Signal Processing*, and acted on the editorial boards of IEEE TRANSACTIONS ON SIGNAL PROCESSING, *IEEE Signal Processing Magazine*, IEEE OPEN JOURNAL OF SIGNAL PROCESSING, *EURASIP Journal on Advances in Signal Processing* and *Foundations and Trends in Signal Processing*.